Chem. Mater. **2000,** *12,* 331−335

Preparation and Characterization of Several High-Area $NiAl_2O_4$ Spinels. Study of Their Reducibility

Yolanda Cesteros,[†] Pilar Salagre,[†] Francisco Medina,[‡] and
Jesús Eduardo Sueiras*,[‡]

*Facultat de Química and Escola Tècnica Superior d'Enginyeria, Universitat Rovira i Virgili,
Pl. Imperial Tarraco1, 43005 Tarragona, Spain*

Received March 15, 1999. Revised Manuscript Received July 16, 1999

A rigorous study was made of the different experimental conditions that affect the obtention of high-area spinels. Some of the key factors in the preparation of $NiAl_2O_4$, such as precipitation and calcination temperatures, have been carefully studied and correlated to the reducibility of the final spinel. All the samples were characterized by X-ray diffraction, nitrogen physisorption, scanning electron microscopy, temperature-programmed reduction (TPR), and X-ray photoelectron spectroscopy (XPS) techniques. Spinels were obtained with high area (110−220 m^2/g) compared with those usually reported. XPS showed that these spinels can be surface reduced. The largest amount of metallic nickel phase was found in the spinel prepared by precipitation at 348 K and calcination at 773 K. This spinel also had the lowest initial temperature of reduction (TPR).

Introduction

The relevance of nickel aluminate spinel as a multidisciplinary material can easily be verified from some of the recently reported studies on the development of chemical-looping combustion,[1] the preparation of high-surface-area materials by an alkoxide route,[2] the mechanism of cation equilibration,[3] the preparation of spinel−mullite composites by sol−gel techniques,[4] the structural bonding between Al_2O_3 and nickel,[5] the influence of residual stresses on metal−ceramic microstructures,[6] the coarsening behavior of alumina−spinel composites,[7] the development of ceramic−metal composites,[8] the rotation−coalescence of particles in composites,[9] the synthesis from α- and γ-alumina-supported oxides,[10] the combustion chemical vapor deposition onto silica substrates,[11] and the preparation of composites from layered double hydroxides.[12]

Spinels are also increasingly being used as catalyst supports since they are stable compounds with strong resistance to acids and alkalis, high melting points, and surface areas in the range 10−100 m^2/g. Several studies on alumina-supported nickel catalysts[13−23] revealed the formation of nickel aluminate spinel, $NiAl_2O_4$. The preparation of nonstoichiometric nickel aluminate compounds leads to the formation of surface NiO which, after reduction, could form a stable nickel supported on a partially inverted spinel structure.[24−29] This form of nickel is more resistant to deactivation by coke formation during re-formation of methane and acetylene

---

* To whom correspondence should be addressed. E-mail: jsueiras@etse.urv.es.

[†] Facultat de Química.

[‡] Escola Tecnica Superior d'Enginyeria.

(1) Jin, H. G.; Okamoto, T.; Ishida, M. *Ind. Eng. Chem. Res.* **1999**, *38* (1), 126.

(2) Platero, E. E.; Arean, C. O.; Parra, J. B. *Res. Chem Intermed.* **1999**, *25* (2), 187.

(3) Backerman, J.; Becker, K. D. *Z. Phys. Chem.-Int. J. Res. Phys. Chem. Chem. Phys.* **1998**, *206* (1−2), 31.

(4) Sales, M.; Valentin, C.; Alarcon, J. *J. Am. Ceram. Soc.* **1997**, *80* (7), 17.

(5) Sun, X. D.; Yeomans, J. A. *J. Mater. Sci. Technol.* **1996**, *12* (6), 421.

(6) Ustundag, E.; Zhang, Z.; Stocker, M. L.; Rangaswamy, P.; Bourke, M. A. M.; Subramanian, S.; Sickafus, K. E.; Roberts, J. A.; Sass, S. L. *Mater. Sci. Eng., A* **1997**, *238* (1), 50.

(7) Tuan, W. H.; Lin, M. C.; Tzing, W. H. *Mater. Chem. Phys.* **1997**, *48* (2), 156.

(8) Rogers, K. A.; Kumar, P.; Citak, R.; Sandhage, K. H. *J. Am. Ceram. Soc.* **1999**, *82* (3), 757.

(9) Wang, S. R.; Shen, P. *Mater. Sci. Eng., A* **1998**, *251* (1−2), 106.

(10) Bolt, P. H.; Habraken, F. H. P. M.; Geus, J. W. *J. Solid State Chem.* **1998**, *135* (1), 59.

(11) Stollberg, D. W.; Carter, W. B.; Hampikian, J. M. *Surf. Coat. Technol.* **1997**, *94−5* (1−3), 137.

(12) Rodeghiero, E. D.; Chisaki, J.; Giannelis, E. P. *Chem. Mater.* **1997**, *9* (2), 478.

(13) Huang, Y. J.; Schwarz, J. A.; Diehl, J. R.; Baltrus, J. A. *Appl. Catal.* **1988**, *36*, 163.

(14) Jacono, M. L.; Schiarello, M.; Cimino, A. *J. Phys. Chem.* **1971**, *75*, 1044.

(15) Cimino, A.; Jacono, M. L.; Schiavello, M. *J. Phys. Chem.* **1975**, *79*, 243.

(16) Zielinski, J. *J. Catal.* **1982**, 76, 157.

(17) Ross, J. R. H.; F.Steel, M. C. *J. Chem. Soc. Faraday Trans. 1* **1973**, *69*, 10.

(18) Bokx, P. K.; Wassenberg, W. B.; Geus, J. W. *J. Catal.* **1987**, *104*, 86.

(19) Salagre, P.; Fierro, J.L. G.; Medina, F.; Sueiras, J. E. *J. Mol. Catal., A* **1996**, 106, 125.

(20) Rodriguez, J. C.; Romeo, E.; Fierro, J. L. G.; Santamaria, J.; Monzon, A. *Catal. Today* **1997**, *37* (3), 255.

(21) Ross, J. R. H.; Steel, M. C. F.; Zeini-Isfahani, A. *J. Catal.* **1978**, *52*, 280.

(22) Rostrup-Nielson, J. R. *Catalysis-Science and Technology*; Anderson, J. R., Boudart, M. Eds.; Springer: Berlin, 1984; Chapter I.

(23) Chen, I.; Shui, D. *Ind. Eng. Chem. Res.* **1988**, *27*, 429.

(24) Al-Ubaid, A.; Wolf, E. E. *Appl. Catal.* **1988**, *40*, 73.

(25) Al-Ubaid, A. *React. Kinet. Catal. Lett.* **1989**, *38*, 399.

(26) Bhattacharyya, A.; Chang, V. W. *Catalysis Deactivation, Studies in Surface Science and Catalysis*; Ed. Delmon, B., Froment, G. F., Eds.; Elsevier: Amsterdam, 1994; Vol. 88.

(27) Peña, J. A.; Herguido, J.; Guimon, C.; Monzon, A.; Santamaria, J. *J. Catal.* **1996**, *159*, 313.

(28) El-Shobaky, G. A.; Al-Noaimi, A. N.; Saber, T. M. *Bull. Soc. Chim. Fr.* **1987**, *6*, 930.

(29) Murthy, I. A. P. S.; Swamy, C. S. *J. Mater. Sci.* **1993**, *28*, 1194.

10.1021/cm990154h CCC: $19.00 © 2000 American Chemical Society
Published on Web 01/27/2000

Table 1. Calcination Conditions To Obtain Several $NiAl_2O_4$ Spinels

gel	calcination temp (K)	calcination time (h)	spinel
E_1	773	5	E_17
E_1	973	5	E_19
E_2	773	5	E_27
E_2	973	5	E_29

hydrogenation processes than when deposited on an inert support.[24,26,29]

Concerning the preparation of the spinels, the sol−gel method of preparing high-surface-area $NiAl_2O_4$ has been reported.[2] The ammonium hydroxide coprecipitation method, described elsewhere,[21] is mainly used to prepare precursors whose spinels are usually obtained by calcination at high temperatures (between 1023 and 1273 K).

In this paper, we discuss how the preparation conditions of the nickel aluminum hydroxide gels and their calcination temperatures affect the final structure of the $NiAl_2O_4$. The samples were characterized by different techniques so that the textural and structural properties could be correlated with the preparation conditions. The study of the reducibility of the different spinels was also studied so that the preparation procedures could be optimized to obtain well-dispersed and stable nickel-supported catalysts.

Experimental Section

Sample Preparation. The nickel aluminate precursors were prepared by coprecipitating a stoichiometric mixture of nickel nitrate and aluminum nitrate solutions ($[Ni^{2+}] = 0.17$ M; $[Al^{3+}] = 0.34$ M) by means of the ammonium hydroxide method described elsewhere.[21] The base (0.6 M NH_4OH) was added at 3 mL/min with constant stirring until the acidity changed from pH 4 to pH 8. The precipitation was carried out at two temperatures: 298 K (gel E_1) and 348 K (gel E_2). The precipitated materials were filtered, washed with deionized water till complete removal of NH_4^+ and NO_3^- ions, and dried overnight in an oven at 373 K.

The $NiAl_2O_4$ spinels were obtained by calcining gels E_1 and E_2 under the conditions shown in Table 1. These four spinels, designated as E_17, E_27, E_19, and E_29, were heated at 673 K under pure H_2 (99.999%) for 6 h (E_17R, E_27R, E_19R, and E_29R). All the samples were characterized by different techniques, shown below.

Air-Free Sampling. The hydrogen-treated spinels were always handled under air-free conditions after the reduction step. The samples were transferred in degassed isooctane and under a hydrogen atmosphere at room temperature. The isooctane surface-impregnated samples were further isolated from the air with a gold film for the SEM study or with sticky tape for XRD monitoring, where a glovebox was used for mounting.

X-ray Diffraction (XRD). Powder X-ray diffraction patterns of the different samples were obtained with a Siemens D5000 diffractometer using nickel-filtered Cu Kα radiation. Samples were dusted on double-sided sticky tape and mounted on glass microscope slides. The patterns were recorded over a range of 2θ angles from 10° to 90°, and the crystalline phases were identified using JCPDS files.

BET Areas and Pore Distributions. BET (Brunauer−Emmett−Teller) surface areas were calculated from the nitrogen adsorption isotherms at 77 K using a Micromeritics ASAP 2000 surface analyzer and a value of 0.164 nm^2 for the cross-section of the nitrogen molecule. The same equipment automatically calculated the pore distribution of the solids, with an accuracy of ±2 Å, for pore diameters between 10 and 3000 Å using the Barrett, Joyner, and Halenda (BJH) method.[30]

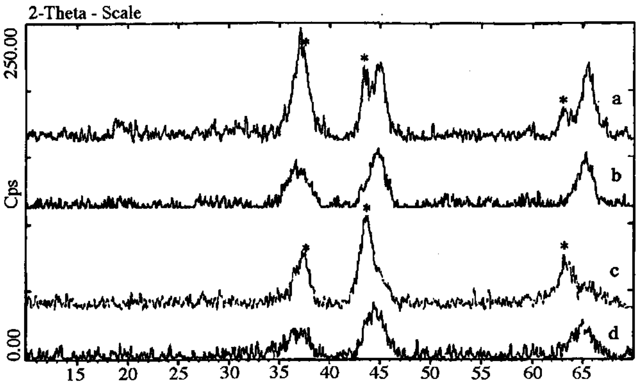

Figure 1. Powder diffraction patterns of the spinels: (a) E_29, (b) E_19, (c) E_27, and (d) E_17. Asterisk indicates NiO

Table 2. Characterization of the $NiAl_2O_4$ Spinels

sample	E_17	E_19	E_27	E_29
cryst phases (XRD)	$NiAl_2O_4$	$NiAl_2O_4$	$NiAl_2O_4$, NiO	$NiAl_2O_4$, NiO
BET areas (m^2/g)	220	154	180	112
$T_R{}^a$ (K)	811	881	771	912

[a] T_R = initial temperature of reduction.

Scanning Electron Microscopy (SEM). Scanning electron micrographs were obtained with a JEOL JSM-35C scanning microscope operating at an accelerating voltage of 30 kV and with a work distance (wd) of 14 mm and magnification values of 650×.

Temperature-Programmed Reduction (TPR). Temperature-programmed reductions were carried out in a Perkin-Elmer TGA 7 microbalance equipped with a 273−1273 K programmable temperature furnace with accuracies of ±1 μg and ±1 K, respectively. Each sample (30 mg) was heated in a 5 vol % H_2/Ar flow (80 cm^3/min) from 293 to 1123 K at 5 K/min. Since it was not possible to carry out the experiments under pure H_2 due to the technical restrictions of the thermobalance, the results were obtained by using 5 vol % H_2/Ar (99.999% pure).

X-ray Photoelectron Spectroscopy (XPS). X-ray photoelectron spectra were recorded on a Leybold LHS 10 spectrometer equipped with a hemispherical energy analyzer and a Mg Kα X-ray radiation source. The spinel samples for XPS characterization were treated by using reduction procedures which were analogous to those described above. They were mounted on a standard sample probe under an inert atmosphere and placed in a preevacuation chamber up to ca. 10^{-5} Torr before they were moved into the main vacuum chamber. The residual pressure in the turbo-pumped analysis chamber was kept below 7×10^{-9} Torr during data collection. Each spectral region was signal-averaged for a given number of scans to obtain good signal-to-noise ratios. Although surface charging was observed on all the samples, binding energies (BE), with an accuracy of ±0.1 eV, were determined by charge referencing with the C 1s line at 284.6 eV. Peak areas of Ni(0) and Ni(II), including satellites, were computed by fitting the experimental spectra.

Results and Discussion

X-ray Diffraction. Figure 1 shows the powder diffraction patterns of the spinels (the crystalline phases of which can be seen in Table 2). NiO is known to interact with Al_2O_3 at relatively low temperatures (673−723 K) to form a surface nickel aluminate.[16,28] The amount formed increases with temperature and time of calcination. In this study, the calcination temperature

---

(30) Barret, E. P.; Joyner, G.; Halenda, P. P. *J. Am. Chem. Soc.* **1951**, *73*, 373.

Table 3. Characterization of the Reduced Spinels

sample	E_17R	E_19R	E_27R	E_29R
cryst phases (XRD)	$NiAl_2O_4$	$NiAl_2O_4$	$NiAl_2O_4$, NiO	$NiAl_2O_4$, NiO
BET Areas	177	116	126	91

used is above these values (773 and 973 K), and therefore a significant amount of aluminate can be expected.

Samples E_17 and E_19, obtained by precipitating the hydroxides at 298 K, have broad peaks characteristic of the $NiAl_2O_4$ phase, whereas samples E_27 and E_29, obtained by precipitating the hydroxides at 348 K, have a new NiO phase in addition to a spinel phase. The 2θ angles (with the relative intensities in parentheses), taken from the JCPDS files, may be summarized as follows: 37.01 (100), 45.00 (65), and 65.54 (60) for the $NiAl_2O_4$ phase and 37.29 (91), 43.30 (100), and 62.91 (57) for the NiO phase. The appearance of different phases is probably related to the temperature of precipitation which can favor both the appearance of small gel particles (confirmed by SEM) and an increase in the differences between the precipitation rates of the two hydroxides. The nickel hydroxide, when heat treated, is more soluble than the aluminum hydroxide,[31] and then the gel obtained during the precipitation procedure loses its homogeneity to some extent. A NiO phase appears after calcination as a consequence of the different precipitation rates when both hydroxides are heat treated.

The results obtained from the diffraction powders of the reduced spinels (Table 3) show the same bulk phases on both the hydrogen-treated and nontreated spinels. No nickel metallic phase was detected by XRD. It may be assumed that the bulks of the spinels remain unchanged after the reduction step. However, the gray-black color of the reduced $NiAl_2O_4$ suggests that the surface layers undergo a nickel reduction. This is in accordance with the XPS results given below.

BET Areas and Pore Distributions. The BET areas of the spinels are shown in Table 2. The spinels E_17 and E_19, obtained from the gels prepared at room temperature, have higher surface areas than the spinels E_27 and E_29, respectively. This is probably due to the fact that, because of the characteristic properties of these gels, a NiO phase (detected by XRD) appears after calcining the gel prepared at 348 K, and therefore these spinels have less surface area.

As expected, when the temperature of calcination increases, the surface areas are rather low due to the higher crystallinity of the spinel and/or the increase in the particle size (sinterization).

Finally, the BET areas for the hydrogen-treated samples are shown in Table 3. The surface areas of these samples are lower than their precursors. The reduced spinels undergo a surface reduction where the small particles of metallic Ni are not detectable by XRD, although they may be responsible for the decrease in the surface area.

At this point the high surface areas of the spinels prepared (110−220 m^2/g), which may offer great possibilities as catalyst supports, should be mentioned. The high area of the reduced spinels (with a maximum of 177 m^2/g) suggests that they may be of interest as catalytic systems with high metallic dispersion.

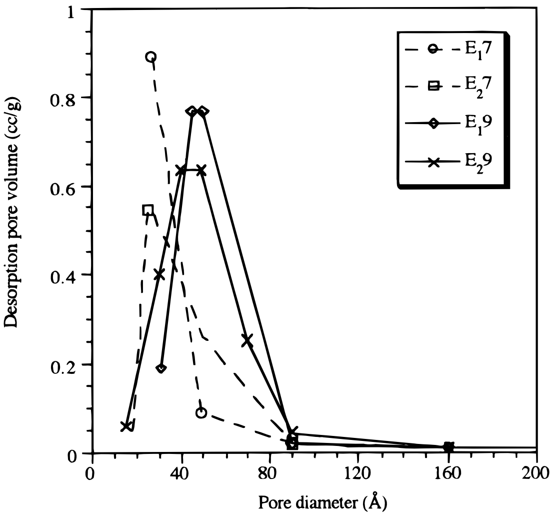

Figure 2. Pore distribution plot for the spinels in the desorption process.

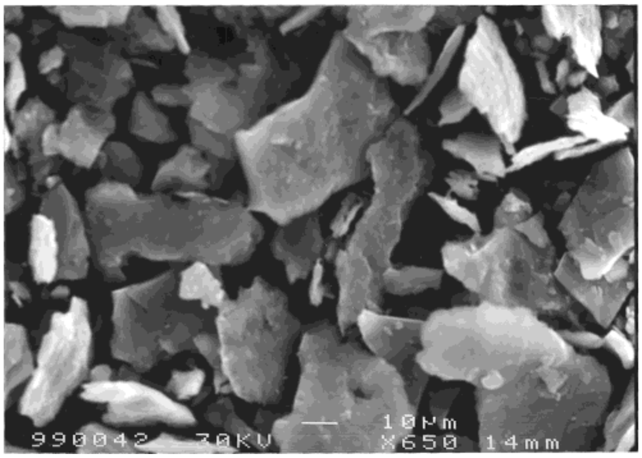

Figure 3. Scanning electron micrograph of the dried gel E_1.

Figure 2 shows the pore distributions as a plot of d*V*/d log(*D*), desorption pore volume (*V*) against the pore diameter (*D*), for the four spinels (BJH method).[30] The pore distribution only shows one maximum in the low mesoporous range with a different value for each spinel. The maximum pore diameter of the spinels prepared by calcination at 773 K is around 27 Å, whereas for the spinels calcined at 973 K it is between 40 and 50 Å.

Scanning Electron Microscopy. The SEM technique was used to confirm the correlation between the particle size of the E_1 and E_2 gels and the precipitation temperature. We estimated here the particle sizes taken from the SEM pictures and the magnification parameters.

Figures 3 and 4 show the scanning electron micrographs of gels E_1 and E_2, respectively. The particle sizes of the gel precipitated at 348 K (E_2) are smaller than those observed from the precipitate at 298 K (E_1). The particle sizes of gel E_2 are mostly in the lower range of 1−25 μm, whereas all the particles of gel E_1 have values around 20−40 μm. These results agree with the micrographs obtained, in a previous study, for the heat-precipitated alumina gels.[32] The particles of those gels precipitated at 348 K were also smaller because the

---

(31) Weast, R. C. *Handbook of Chemistry and Physics*, 64th ed.; CRC Press Inc.: Boca Raton, FL, 1984; Section B.

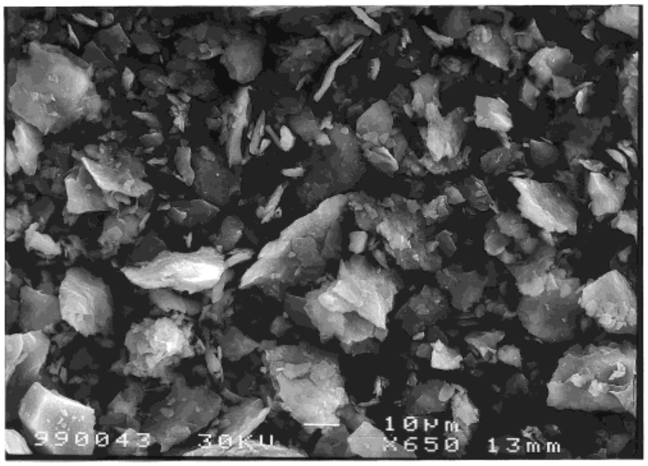

Figure 4. Scanning electron micrograph of the dried gel E_2.

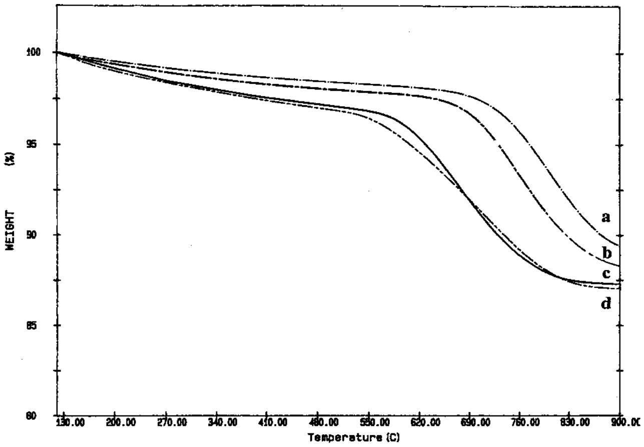

Figure 5. 5. TPR plots of the $NiAl_2O_4$ spinels: (a) E_29, (b) E_19, (c) E_17, and (d) E_27.

precipitation was slower. The fact that gel E_2 has smaller particles than E_1 should lead to a more efficient mixing of the hydroxides, higher yields of spinel formation, and consequently larger crystallite sizes. This was confirmed because the BET surface areas obtained for spinels E_27 and E_29 were lower than those for spinels E_17 and E_19.

Temperature-Programmed Reduction. The reducibility of the spinels was studied by temperature-programmed reduction. The great interest of these TPR studies is to establish correlations between the reducibilities of the spinels and the preparation conditions. Figure 5 shows the TPR profiles of spinels E_17, E_19, E_27, and E_29. Although there seems to be an initial baseline drift, a general weight loss can be observed from 500 °C (773 K) onward. Table 2 shows the values of the initial reduction temperature for all samples.

The initial reduction temperature of the spinels decreases in the following sequence:

$$E_29 > E_19 > E_17 > E_27$$

The spinels prepared from the calcination at 973 K show a higher value of the initial reduction temperature due to their larger crystallite sizes. This makes the reduction process more difficult. In contrast, the spinels with higher BET areas and smaller particle sizes, obtained at lower calcination temperature (773 K), start their reduction earlier. These results agree with those obtained by Peña et al.,[27] who reported an initial reduction temperature around 973 K for a crystalline spinel prepared by calcination at 1173 K. Other authors[33] also confirmed the reducibility dependence of $NiAl_2O_4$ on the previous calcining temperature.

Table 4. XPS Binding Energies and Ratio of Surface Nickel Species

sample	BE (eV) Ni $2p_{3/2}$		Ni^{2+}/Ni	surface reduction degree (%)
E_17R	854.0	852.8	1.27	44
E_19R	854.7	853.5 (sh)		
E_27R	854.2	852.8	1.08	48
E_29R	854.9	853.5 (sh)		

Comparing E_17 and E_27 (calcined at 773 K), we observed that spinel E_27 starts reducing earlier, probably because the different precipitation rates of the nickel aluminum hydroxide gels prepared at 348 K favor the presence of a considerable amount of NiO (detected by XRD) after the calcination procedure. The NiO particles interact considerably with the spinel phase,[34] and only small amounts of NiO can be reduced more easily. On the other hand, the reduction procedure for samples E_19 and E_29 is different because the E_19 starts to reduce first. This may be due to the larger crystallite size of spinel E_29 and its lower content of NiO (as shown by XRD), which is probably covered by the spinel after the thermal treatment at 973 K. As a result, the spinel-decorated NiO makes it difficult for E_29 to reduce further.

X-ray Photoelectron Spectroscopy. Table 4 summarizes the XPS results after the "in situ" hydrogen treatment for the four spinels. From the BE values of Ni $2p_{3/2}$, we can observe only one peak at about 855 eV for either E_19R or E_29R. This indicates that the surfaces of these samples mainly contain nickel in +2 state.[13,24,29] Both samples also have a small shoulder at 853.5 eV which can be assigned to an incipient metallic nickel phase.

Samples E_17R and E_27R show a broad band with two maxima. One, around 854 eV, is due to the Ni^{2+}, and the other, with a lower BE value (852.8 eV), is characteristic of the nickel phase.

The surface Ni^{2+}/Ni content ratio obtained from the deconvolution of the experimental curve indicates a considerable degree of surface reduction for the spinels obtained at lower temperature, i.e., 44% for E_17R and 48% for E_27R (see Table 4). This agrees with the lower initial temperature of reduction of the E_27 sample (see Table 2).

It should be pointed out that metallic nickel was observed under our milder reduction conditions while other studies from the literature required the use of argon ion sputtering,[24,29] a higher reduction temperature (up to 973 K), or a longer time of reduction.[27] The significant amount of surface-reduced nickel obtained in this study may be related to the small crystallite sizes in our spinels prepared at 773 K.

---

(32) Cesteros, Y.; Salagre, P.; Medina F.; Sueiras, J. E. *Chem. Mater.* **1999**, 11(1), 123.

(33) Numaguchi. T.; Eida, H.; Shoji, K. *Int. J. Hydrogen Energy* **1997**, *22* (12), 1111.

(34) Jinxiang, L.; Lixiu, Y.; Xuanzhen, J.*Thermochim. Acta* **1991**, *178*, 9.

Conclusions

The precipitation and calcination temperatures of the nickel aluminum hydroxide precursors of the spinels were correlated with the reducibilities of the final $NiAl_2O_4$. XRD showed the presence of the spinel phase in all samples and a NiO phase on the spinels from the precursors precipitated at 348 K. The effect of the precipitation temperature favors the formation of a less homogeneous gel with smaller particle sizes (observed by SEM). The XRD of the reduced $NiAl_2O_4$ indicates that the bulk spinel structure remained unchanged after the hydrogen treatment, while the XPS technique revealed a surface reduction of the spinels. The degree of surface reduction was highest in the spinel obtained from the gel precipitated at 348 K and calcinated at 773 K. This agrees with the TPR results. The calcination temperature and the hydrogen treatment produce a decrease in the surface area.

Consequently, the high-area spinels prepared in this work can be surface reduced and may be used in systems of catalytic interest in hydrogenation reactions and in the preparation of more resitant reduced catalysts.

CM990154H